RSC Advances

ROYAL SOCIETY OF CHEMISTRY

www.rsc.org/advances

Cite this: DOI: 10.1039/c0xx00000x

www.rsc.org/xxxxxx

PAPER

Potential in vitro and in vivo colon specific anticancer activity on HCT-116 Xenograft Nude mice model: Targeted delivery using enteric coated folate modify nanoparticles

*Renuka Khatik[1], Pankaj Dwivedi[1], Vijayabhaskar Reddy Junnuthula[1], Komal Sharma[1], Krishna Chuttani[2], Anil Kumar Mishra[2], Anil Kumar Dwivedi[1]**

Abstract: The aim of the study was to develop a drug delivery system for specific targeting in colon cancer. We have developed Eudragit S-100 (ES) coated folic acid (FA) conjugated gliadin (Gd) delivery system for the effective targeting to the over expressed folate receptors (FRs) in colon cancer. The FA conjugate with Gd (FA-Gd) was synthesized and characterized by FTIR and 1H NMR, this developed conjugated was used to prepare curcumin (CU) loaded nanoparticles (NP) by desolvation method. FA-CU-GdNP was further coated with ES and ES-FA-CU-GdNP was obtained. The ES-FA-CU-GdNP were also capable of inducing cell caspase dependent apoptosis in Caco-2 cell lines and exhibit DNA intercalating activity. In therapeutic experiments the ES-FA-CU-GdNP was administered orally to HCT-116 tumor bearing nude mice. In vivo data of bio-distribution showed that ES-FA-CU-GdNP delivered maximum amount of NP in the colon and tumor, respectively after 12 hours, reflecting its targeting potential to the colon and tumor. Gamma scintigraphy study suggested that ES-FA-CU-GdNP at low pH and released NP slowly at pH 7.4 in the colon. These studies provide evidences that ES-FA-CU-GdNP holds promise to address over-expressed FRs in colorectal cancer and were found to be safe for oral administration for prolonged duration.

Graphical abstract:

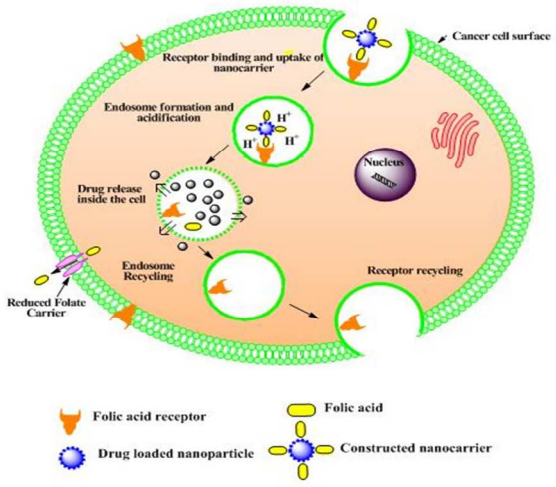

Graphic diagram representing the Receptor-mediated endocytosis of FA-CU-GdNP.

1. Introduction

Cancer is a principal cause of distressing and death, with more than 10 million people being diagnosed with the disease every year [1, 2]. The most often treatment of cancer is chemotherapy or the surgical procedures, which have connection with number of disadvantages, i.e. it damage healthy tissues leading to systemic toxicity, multidrug resistance, nonselective distribution of drugs and adverse side effects [3, 4]. Nanotechnology, one of the efficacies technologies which have been adapted by the medical experts can pave the way to overcome the problems related to safe drug delivery. Sustained release of drugs might overcome problems associated with high dose related toxicity and drug resistance which can also be used as new concept in chemotherapy [2]. The efficacy of the traditional medicines open up new opportunity for future cancer therapies [5]. In this consideration, the upcoming anticancer drug of natural herbal extract; curcumin (CU) gives a solution to the obstacles involved in chemotherapy by showing safety and chemopreventive effect which can be loaded into a nanoparticles (NP) that delivers the drug into malignant cell [6].

CU, a natural hydrophobic phenolic compound, isolated from the rhizome of Curcuma longa (turmeric), has a wide spectrum of healthy functions and pharmacological activities [7, 8]. It also exhibit anticarcinogenic properties [9] and sensitization of tumor cells for chemotherapy and radiation with low intrinsic toxicity [10, 11]. With all such advantages CU has limited usage due to its poor aqueous solubility, and thus, minimal systemic bioavailability. Various formulations of CU were investigated in an effort to improve its oral bioavailability, including encapsulation in liposomes [12, 13], CU complexed with phospholipids [14] and cyclodextrin [15]. NP has also been reported to improve its bioavailability [16]

In this view, one of the approaches to achieve enhanced bioavailability of CU may be to encapsulate it with natural polymers (e.g., polysaccharides, glycoprotein, polypeptides, and lipids). The natural polymers are less toxic and safer than synthetic polymers [17, 18]. In addition, natural polymers or glycoprotein are promising carriers for delivery and controlled release of drugs, because they are biodegradable, nontoxic, and stable [19]. Gliadin (Gd), a plant protein contains neutral amino acids, which enhance hydrogen bonding with the mucus layer, and lipophilic amino acids that support hydrophilic interactions [20, 21]. Gliadin (Gd) has been reported to serve as an enzyme carrier of superoxide dismutase which protects the acid degradation of the enzyme and allows it to release in intestine; this property can be used to deliver the maximum amount of drug to the colon. Gd has previously been used for the preparation of NP for drug delivery and controlled release applications [22]. The stability of Gliadin nanoparticles (GdNP) increased when chemically cross-linked with gluteraldehyde. Although various drugs have been loaded into GdNP for delivery and controlled release, GdNP loaded with anticancer drugs have not yet been fully explored.

In order to improve the effectiveness and uptake of the NP into specific targeted cells, target-specific ligands, such as FA can be used. FA is a stable compound having high affinity towards FRs [23, 24] which are over-expressed on many human epithelial cancer cell surfaces especially in colon. The targeting ability of drug can be improved by conjugating the drug delivery carrier with FA [25, 26]. FA conjugates delivery systems, which are covalently derivatized via folate's γ-carboxyl moiety, can maintain a high affinity to the FRs [27]. Later, the unligated FRs may recycle to the cell surface to move more FA conjugates in the cell cytoplasm [24]. The mechanism of endocytosis mediated by FRs.

In this scenario, the choice of a receptor mediated targeted delivery has more advantages for the efficient intracellular delivery on the one that relies on cell membrane markers. Colon cancer cells have FA deficiency hence arrest more FA conjugated NP than the normal cells [1, 28-30]. To date, NP has been widely functionalized with ligands and antibodies to target FRs on cancer cells.[31, 32]

In the present investigation, FA rich FA-CU-GdNP, has been prepared and found to be more effectively targeting the over expressed FRs in colorectal cancer when compared to CU-GdNP. We can conclude that the FA-CU-GdNP have higher cancer targeting potential on tumor bearing nude mice. We also determined the pharmacokinetics, biodistribution and tumor growth inhibition study. We then evaluated the potential of these FA-CU-GdNP coated with Eudragit S-100 (ES) in inhibiting angiogenesis and suppressing the growth of colon tumor in vitro and in vivo.

2. Results

2.1. Conjugated FA-Gd characterization by FTIR

FA conjugation to Gd was accomplished by a new application for the Mitsunobu reaction. The FTIR spectra of the FA modified Gd showed the typical peaks (Figure.2). The O-H broadened stretching band in the region 3281 cm-1 was found. IR spectra of the FA conjugated Gd, shows the characteristic absorption bands at 1063 cm-1 which were due to C-O stretching vibrations of ester formed. The IR spectra of FA conjugated Gd shows C=O stretching at nearly 1630 cm-1.

2.2. NMR Spectroscopic Characterization of FA Conjugation to Gd

Chemical conjugation of FA with Gd was also confirmed by 1H NMR spectroscopy. 1H NMR spectra showed that the FA was successfully conjugated to Gd. In 1H NMR (300 MHz) of FA conjugated Gd (Figure.3), the appearance of aromatic proton (Ar-H) from δ 6.7 to δ 7.9 indicates the presence of FA moiety in our product while C-H, -CH2 protons was found from δ 0.8 to δ 2.2, some -CH2 protons present near -N- were shifted and were present on δ 3.7 to δ 4.5 and –OH protons of FA conjugated Gd appeared from δ 5.2 to δ 5.3.

2.3. Differential Scanning Calorimetry (DSC)

Interaction of CU with Gd was also confirmed by DSC, which gives information about compatibility of CU with Gd. DSC thermograms of CU, Gd and CU-Gd physical mixture are shown in (Figure.4) in which a sharp endothermic peak at 183 °C has been observed during DSC of CU due to dehydration of the crystalline network, where in the thermo-gram of the Gd, broad hump near 70-75°C emerged. However, in the case of CU-Gd physical mixture shows no difference in their physical characteristics and the peak emerged at their regular place at 70-75°C for Gd and 183°C for CU revealing on interaction between these two.

2.4. Characterization of ES-CU-GdNP and ES-FA-CU-GdNP

The mean particle size of ES-GdNP, ES-FA-GdNP, ES-CU-GdNP and ES-FA-CU-GdNP was found to be 98.3 ± 3.5 nm, 112.4 ± 8.6 nm, 137.2 ± 4.1 nm and 249.3 ±7.2 nm with PDI of 0.131, 0.127, 0.191 and 0.175 respectively. The zeta potential of ES-GdNP, ES-FA-GdNP, ES-CU-GdNP and ES-FA-CU-GdNP was found to be -8.3 ±1.2 mV, -21.3 ± 1.6, -10.7 ±2.0 mV and -27.1 ±1.8 mV respectively with narrow size distributions measured by DLS. The data has been illustrated in Table1. %EE in ES-CU-GdNP was found to be 49.4 ±3.8% whereas in ES-FA-CU-GdNP there was increase in the %EE (53.2± 4.1%). In Figure.5 (A and B) show the morphological characteristics of CU-GdNP and FA-CU-GdNP, respectively, by TEM study. Surface modification is signified by the incessant opaque and irregular layer of FA-CU-GdNP (Fig 5, B) over CU-GdNP.

2.5. *In vitro* Release study

The *in vitro* release profile of CU from ES-CU-GdNP and ES-FA-CU-GdNP was studied by using pre activated dialysis bag (Sigma; cut off MW-12 KD) at different pH 1.2, 7.4 and 6.8 while the temperature of the medium was kept at 37°C. The *in-vitro* release of CU was released instantly within 6 h. It was observed that there was no drug release up to 2-3 hours in case of both the ES-CU-GdNP and ES-FA-CU-GdNP, whereas drug initiates to be released only after 3 hours at SIF pH 7.5. This can be explained by the fact that the ES polymer contains carboxyl groups that ionize from neutral to alkaline media. As the ionization takes place, integrity of the coating is disturbed and releases the NPs. Further the release conducted in the presence of rat caecal and colonic contents having pH of 6.8, where the total cumulative amount of CU released from ES-CU-GdNP, drug release was found to be 52.23% ± 2.16%, 64.09 ± 2.32% and 68.3% ± 2.9% at the end of 8, 12 and 24 hours, respectively; in the case of the ES-FA-CU-GdNP, drug release was found to be 46.44% ± 1.39%, 58.16% ± 2.07% and 63.23 ± 2.17% at the end of 8, 12 and 24 hours, respectively. (Figure.6), results indicate that ES-CU-GdNP and ES-FA-CU-GdNP releases the maximum amount of CU in the colon environment due to the sustained release from the matrix system.

2.6. *In Vitro* uptake Studies

The in vitro uptake study has been conducted to scrutinize the significance of prepared ES-FA-CU-GdNP over ES-CU-GdNP. The study was conducted on Caco-2 cells by flow cytometry study and the uptake intensity of ES-CU-GdNP and ES-FA-CU-GdNP over blank was measured. Figure.7 shows the macrophage uptake of ES-CU-GdNP and ES-FA-CU-GdNP in Caco-2 cells by flow cytometry study. The mean fluorescence intensity shows almost two times (>2.127) enhanced uptake of ES-FA-CU-GdNP over ES-CU-GdNP in caco-2 cell lines revealing the significantly higher ($P<0.05$) uptake of ES-FA-CU-GdNP in comparison with ES-CU-GdNP as the presence of folate receptors might be mediating the uptake.

2.7. Apoptosis studies

Toward finding the possible reason of how ES-CU-GdNP and ES-FA-CU-GdNP could kill cancer cells, we have analyzed the apoptosis induction in ES-CU-GdNP and ES-FA-CU-GdNP treated colon cancer cells such as Caco-2. Apoptosis is one of the major cell death pathways induced by anticancer agents and we have evaluated apoptosis inducing effects of ES-CU-GdNP and ES-FA-CU-GdNP by Annexin V/Propidium iodide (PI) binding. As can be seen in Figure.8, The fraction of apoptotic cells was higher in case of cells treated with ES-FA-CU-GdNP than with ES-CU-GdNP or with Plain CU, the ES-FA-CU-GdNP increased the percentage of apoptotic cells in Caco-2 cells from 0.40% in

control While CU had very few cells i.e. 9.69% in apoptotic phase, the ES-CU-GdNP and ES-FA-CU-GdNP had shown to 16.82 % and 54.70% in treated cells. From the above data it is evident that ES-FA-CU-GdNP truly induced apoptosis specifically in colon cancer cells irrespective of ER status and did not induce apoptosis in normal cells.

2.8. Cytotoxicity Study

The dose dependent cytotoxicity of the NP was determined by MTT assay 33. Caco-2 cells were plated with plain CU, ES-CU-GdNP and ES-FA-CU-GdNP at different concentrations and cultured for 24 hr with 5% CO2 at 37°C and the cytotoxicity for cells was determined by MTT assay. The percentage cell viability of different NP with different concentration was found to be significantly less in comparison to plain CU. The blank formulations ES-GdNP and ES-FA-GdNP showed slight cytotoxicity (less than 10%) revealing the safety of the excipients used. The cell viability at 5µM,10µM, 20µM and 40µM concentrations was estimated and the results revealed that the viability of cells exposed to ES-FA-CU-GdNP was less than the cells exposed ES-CU-GdNP At higher concentration (40µM) ES-FA-CU-GdNP and ES-CU-GdNP showed 16.4 ± 0.92 % and 22.7 ± 1.13 % of cell viability respectively, at 20µMol ES-FA-CU-GdNP and ES-CU-GdNP showed less than 40% of cell viability whereas at lower concentration (10 µM) ES-FA-CU-GdNP showed 33.5±1.67 % and ES-CU-GdNP showed more than 45% of cell viability. The data has been represented in (Figure .9).

2.9. Analysis of pharmacokinetic parameter after oral administration

The overall pharmaceutical targeting efficacy of the CU loaded surface engineered ES-FA-CU-GdNP were evaluated in HCT-116 tumor bearing nude mice. The plasma concentration profiles of equivalent 25.0 mg/kg body weight CU after oral administration of the free CU, ES-CU-GdNP and ES-FA-CU-GdNP and pharmacokinetic parameters were determined using non-compartment modeling as summarized in Table 2 (Figure.10). Higher MRT and higher AUC0–∞ of ES-FA-CU-GdNP were approximately 3.8 folds higher, respectively as compared to free CU i.e. (14.65571±3.52 h, 108372.5±102.34 ng/h/mL) as compared to ES-CU-GdNP (11.4301±2.14h, 8123.57±85.1ng/h/mL) were approximately 2.9 folds higher as compared to free CU. and CU (5.605±2.57 h, 2794.44±61.13 ng/h/mL) respectively. ES-CU-GdNP exhibited a rapid increase in the plasma level, which reached a maximal plasma concentration (Cmax=847.067±29.67 ng/mL) than that of ES-FA-CU-GdNP (Cmax= 706.7±24.89 ng/mL) and CU (Cmax=537.47± 15.05 ng/mL). It clearly evinces the enhanced pharmacokinetics with better bioavailability and more prolonged retention in systemic circulation than that obtained on administration of ES-CU-GdNP and plain CU.

2.10. Tissue distribution study

A tissue distribution study was carrying out to evaluate the in vivo CU release in different parts of the GIT from enterically protected enteric coated NP. The results of drug distribution from ES-CU-GdNP and ES-FA-CU-GdNP in the upper GIT after oral administration are displayed in Figure.11 respectively. Entire GIT parts were homogenized, and the content of CU was quantitatively evaluated by using an HPLC assay previously described. The free CU accumulates progressively in stomach, where upto 72.90.14% of dose is localized after 2 h administration whereas only 1.91% of CU was found after 6 h. In all cases the CU concentrations were considerably higher for the ES-FA-CU-GdNP than for the ES-CU-GdNP, CU concentration in colon and tumor tissue after 12 hours was observed to be 9.34 and 11.6 (ES-CU-GdNP) and 8.26 and 30.44 µg CU/g tissue (ES-FA-CU-GdNP), respectively.

2.11. γ-Scintigraphy study

The gastric transit and colon arrival time of designed NP bearing 99mTc-DTPA in nude mice were recorded using γ-scintigraphy. The mean gastric emptying time of the formulation was found to be 1.50±0.17 hrs, mean intestinal transit time was calculated to be 3.20±0.22 hrs and mean colon arrival time was 6.60±0.27 hrs (Figure.12) after the administration of the NP.

2.12. Assessment of anti-tumor cancer targeting efficiency.

The percentage body weight changes of the HCT-116 tumor bearing nude mice model after oral administration of the CU loaded formulations was calculated upto 35 days as showed in Figure. 13(A). It clearly suggests that the developed formulations do not affect the body weight of the nude mice, while in case of the normal saline treated group the loss of body weight was observed These results further confirmed that the higher tumor treatment potential infatuated by the ES-FA-CU-GdNP.

The in vivo tumor targeting efficacy was assayed on HCT-116 tumor bearing nude model and the starting tumor size was approximately 100 mm3 for all dose receiving groups of the developed ES-CU-GdNP and ES-FA-CU-GdNP as well as normal saline and plain CU. The tumor volume (mm3) was 129.01, 118.7, 102.5 and 90.5 in case of normal saline, free CU, ES-CU-GdNP and ES-FA-CU-GdNP at 5th day. The size of the tumor volume (mm3) was reduced to 79.8 and 43.89 in 35th days after treatment with ES-CU-GdNP and ES-FA-CU-GdNP formulations, respectively [Figure. 13(B)]. (**P < 0.001 for ES-FA-CU-GdNP versus control and CU). (* # P<0.01 for ES-CU-GdNP versus control and ## P<0.05 Depicts comparison of ES-CU-GdNP versus CU.

3. Discussion

NP derived from natural sources has been established as of enormous profit for drug delivery and cancer therapy 34, 35. The aim of this present investigation was to target the CU to the colon which was delivered by encapsulating in ES-FA-CU-GdNP. The motive of specific delivery of CU to colon for targeting the colon cancer was not achievable by delivering the CU by unmodified simple CU-GdNP, due to unspecific delivery and loss of CU in undesired area; some specific targeting legend which can be exploited to deliver CU to colon is required. To fulfill our requirement the FA, which has been reported previously 26 for binding to the FRs present on colon has been exploited. The FA binding ability with the FRs over expressed on colon in malignancy allows for the specific delivery of CU. FA, a stable, inexpensive, and generally poorly immunogenic chemical was conjugated with Gd. Gd was conjugated to FA molecules using a new application for the Mitsunobu reaction. The formation of FA-Gd was confirmed by FT-IR and NMR studies, which clearly indicates the conjugate formation. The FA-Gd conjugate was further used for preparing the FA-CU-GdNP, a FA rich delivery system by desolvation method, this system has been further coated with ES in order to specifically target the CU in colon 26, 36. The FA bind to cell surface FRs with nanomolar affinity. After binding, the cell membrane introverts and pinches off to form an endosome. As the endosomal partition acidifies, the folate conjugate and CU discharges from the receptor into the cytosol. Although the reduced folate carrier is thought to be present in virtually all cells, In contrast, membrane bound FRs largely reprocess back to the cell surface, allowing for

deliverance of further folate-linked drugs into the cell 37. To examine the targeting specificity of ES-FA-CU-GdNP; ES-CU-GdNP; blank ES-GdNP have also been prepared by the same desolvation method. TEM micrographs confirmed the nanosize range show clearly coated spherical shaped ES-FA-CU-GdNP and the change in the amount of surface charge alters the dielectric state of ES-FA-CU-GdNP, consequently resulting increases of the zeta potential values. The % EE of ES-FA-CU-GdNP was found to be slightly higher than ES-CU-GdNP. The compatibility of Gd with CU was confirmed by the DSC and was found attuned. The in vitro CU release profiles of the ES-FA-CU-GdNP and ES-CU-GdNP in 24 h are shown in Figure 6. ES-FA-CU-GdNP and ES-CU-GdNP, there was no release of CU at pH 1.2 as anticipated; however, the release was observed when the pH of the medium was adjusted to 7.4 or 6.8. This clearly exhibits that maximum fraction of CU was available in colon, this pH- dependent solubility of ES was exploited to avoid the rapid dissolution of CU during the initial transit of the ES-FA-CU-GdNP through the gastric cavity. The drug release from the ES-FA-CU-GdNP shows similar behavior to that of ES-CU-GdNP apart from the little slower rate due to FA conjugated on the surface of CU-GdNP which provides the possibility to often fight against cancer cells, resulting in the decreased cancer cell viability (shown in the segment of in vitro cytotoxicity below) 38. Conventional dissolution testing is less likely to accurately calculate in-vivo performance of colon specific delivery systems triggered by bacteria residing in the colon due to factors related with colon's environment such as insufficiency of fluid, decreased motility, and presence of micro flora 39. Hence, release studies were performed in an alternate release medium (PBS 6.8 with rat cecal contents). After 12 h the percent CU released in the SCF (pH 6.8) containing 4% rat cecal contents with enzyme initiation at 37 °C was found to be 68% and 63% for the formulation ES-CU-GdNP and ES-FA-CU-GdNP respectively. Thus, the step release of CU from matrix at pH 6.8 of colonic fluid was due to diffusion through nanopores of polymer network or degradation of polymer matrix by colonic bacteria. Significantly higher ($p<0.001$) uptake of ES-FA-CU-GdNP over ES-CU-GdNP in Caco-2 cell lines generates interest that still there is scope of enhanced localization of ES-FA-CU-GdNP in colon macrophages. ES-FA-CU-GdNP was able to localize higher intensity of fluorescence inside the cells compared to ES-CU-GdNP because of better interaction with FRs on macrophages confirmed by apoptosis.

Apoptosis is a key regulator of physiological growth control and regulation of tissue homeostasis but it is highly deregulated in cancer. Implementation of apoptosis is regulated by excess of cell signaling pathways and recent chemotherapeutic agents solely exhibit their action by targeting these signaling pathways. The enhanced therapeutic ability of dual effect of formulation with distinct cellular targets is able to hit signaling cascades simultaneously, thus ultimately causing enhanced apoptosis.

Cytotoxicity of ES-FA-CU-GdNP was found to be significantly ($p < 0.001$) higher than ES-CU-GdNP and CU both. This effect could have been attributed to preferential binding of FA with FRs on the Caco-2 cells thus inhibiting up-regulated cell growth. The results illuminate low toxicity of the blank NP as well as ability of ES-FA-CU-GdNP to preferentially target CU to colon cancer cells. The cell cytotoxicity studies reveal negligible cytotoxicity of both blank ES-FA-GdNP and GdNP in Caco-2 cells lines indicating that the FA is not adding any kind of further cytotoxicity to the formulation instead facilitating the uptake without any damage. Having dual advantage of the surface modified NP by releasing the CU in the colon as well receptor mediated uptake by the cancer cells, its application for the targeted delivery of bioactive is in offing.

Our experimental conclusions that FA causes ligand specific internalization and enhanced endocytosis of NP which leads to superior cytotoxicity can also are supported by related findings of various research groups. Folate decorated poly (lactide)–vitamin E TPGS nanoparticles for the targeted delivery of paclitaxel was synthesized by the group of Pan et al. in which they have shown the improved advantages of the NP versus the pure drug in achieving enhanced therapeutic effect 40.

Namely, the behavior of NP in vivo correlated well with their in vitro interaction with tumor cells. Indeed, the in vitro antitumor activity of NP were tested by using MTT method was performed after cell directly interacted with free CU or NP formulation. In this process, the cellular uptake and the resulting intracellular release play important role. But in vivo, NP having anti-tumor effect is a complex biological process, in which CU first should be targeted to the tumor site and then use inhibitory effect on tumor cells, determined factors that are greatly different from that in vitro.

One of the major interests lying in ES-FA-CU-GdNP is to improve in vivo bioavailability of CU. Interestingly, our results showed ES-FA-CU-GdNP and ES-CU-GdNP is 3.8 and 2.9-folds more AUC0–∞ compared to plain CU respectively which improved bioavailability.

The biodistribution studies indicated that ES-FA-CU-GdNP reached the tumor and were more effective in treating colon tumors as compared to ES-CU-GdNP and the free CU. This may be due to ligand mediated uptake of ES-FA-CU-GdNP in the tumor and releases the drug in tumor instead of colon. The reason for this amount of drug in colon may be due to the larger number of NP uptake from the tumor surface via receptor mediated endocytosis and few of the NP are also expected to reach through tumor leaky vasculature by FRs, a human colon adnenocarcinoma, could be as large as 400 nm and the NP size well below this pore size i.e. in the size range of 150 to 335 nm, hence it could be the reason for successfully achieving the targeting strategy.

The most useful technique, to date, to evaluate in vivo behavior of dosage forms in animals and humans is external scintigraphy or γ-scintigraphy, After testing the in vitro colon targeting behavior of ES-FA-CU-GdNP, it was worthwhile to evaluate the in vivo behavior in terms of residence time of NP in different parts of GI tract. The interesting fact in the transit of the material is that during the initial hours of the study the NP remains firm which may cause fast transit and as the time passed the rigidity of the NPs became weaker due to penetration of solvent and that led to slow transit through rest of the GI tract. 41 also observed gastric emptying values from 0.4 to 4.4 hrs with multiparticulate radiolabeled NP administered to human volunteers

It is clearly seen from the captured scintigraphs that little amount of the radiolabelling was released in the stomach (Figure 12.a). This corresponds to effective enteric coating to the NP. It is evident from the scintigraph taken after 3 hrs (Figure 12.b) that small quantity of tracer was released in the small intestine during 1.85 to 3.20 hrs time period. The NP remains intact as it descends down through the small intestine. The radiolabeled tracer activity, which was released in small intestinal environment, is visible around the NP. After 3.0 hrs as the formulation entered into ascending colon, release of the tracer was increased (Figure 12.c). It is due to a change in the pH of the lower GIT leading to dissolution of enteric coating and thus release of the tracer. After 5 and 6 hrs, the formulation remained in the ascending colon but the release of radioactivity from NP was considerably improved as the coating dissolved with time in the colon but its shape was

distorted with the liberation of considerably higher amount of tracer. After 11-12 hrs (Figure 12.d) the formulation entered into transverse colon leaving the ascending colon filled with the tracer released. The NP was completely disintegrated after 10 hrs (Figure 12.e) and after 24 hrs; the movement of the radiolabelling NP in intact form from stomach and small intestine to the colon without the tracer being released and complete degradation of the network in the colon reveals the efficiency of this pH dependent system.

The in vivo anticancer study once again indicated that compared with the CU, the ES-CU-GdNP and ES-FA-CU-GdNP exhibited a notably enhanced anticancer efficacy. There is significant difference was observed between mice treated with saline and CU with NP mice (Figure.13A and B) showed that the relative body weight and the tumor volume in the tumor bearing nude mice were obvious different among the various experiment groups. Both saline and CU showed similar anticancer activities within 30-35 days. Neither saline nor CU had any measurable influences on tumor growth, in both groups the tumor volumes and weights increased rapidly. For nude mice treated with ES-FA-CU-GdNP, the decrease in body weight was limited and a complete tumor regression was observed for over 50% of mice compared with the saline or CU groups. The increases of body weights in saline-treated mice and CU-treated mice were because of the incredible increases in tumor volume. The design of appropriate ES-FA-CU-GdNP and ES-CU-GdNP are beneficial.

4. Materials and methods

4.1. Materials

Curcumin (CU) and Gliadin (Gd) were purchased from Merck India Ltd., Mumbai (India). Sodium azide-flourescin isothiocynate (FITC), fetal bovine serum (FBS), 3-(4,5-dimethylthiazol-2-yl)-2,5-diphenyl tetrazolium bromide (MTT), Tween 80 and Sorbitan trioleate (Span85), Folic Acid(FA),1-(3-dimethylaminopropyl)-3-ethylcarbodiimide hydrochloride (EDC), Sodium chloride, N, N'-Dicyclohexylcarbodiimide (DCC), 4-Dimethylamino pyridine (DMAP) were purchased from Sigma Aldrich (St. Louis, USA). Triethylcitrate, Dialysis bag (cut off mol. wt. 12000 Dalton) were purchased from Himedia (Mumbai, India). HPLC grade acetonitrile and methanol were purchased from Spectrochem India. Well plates for cytotoxicity and uptake studies were from Greiner Bio One 110 (Frickenhausen, Germany). All other chemicals used were of analytical grade. Triple distilled water was used throughout the study prepared by Milli- Q plus 185 purification system (Bedford, Massachusetts).

4.2. Culture Cell

Coco-2 cells were maintained in Roswell Park Memorial Institute (RPMI 1640, Merck) supplemented with 10% FBS (Merck) and 1% Antibiotic-Antimycotic Solution (Merck) at 37ºC in a humidified incubator with 5% CO2. All stock solution of solutions of the compound were prepared in cell culture grade DMSO and stored in −20 ºC. Human colorectal carcinoma cell line HCT116 was kindly gifted by Dr Bert Vogelstein, Johns Hopkins University. The cells were grown in McCoy's 5A media (Sigma Aldrich) supplemented with antibiotics, L-glutamine and 10% Fetal Bovine Serum (Gibco BRL) at 37 ◦C. All NP were diluted in culture media prior to use in experiments.

4.3. Synthesis of FA conjugated Gd

Gd was esterified by FA using the application of Mitsunobu reaction giving the FA conjugated Gd [42]. FA and Gd was refluxed in presence of tetrahydrofuron (THF), Diethyl azodicarboxylate (DEAD) and triphenylphosphine (Ph3P); the product obtained was dialyzed for purification in two sep; firstly against phosphate buffered saline (PBS pH 7.4) for 3 days and then against water for 4 days. The FA-Gd conjugate was collected by lyophilization and kept for further use. The schematic representation of the reaction has been illustrated in Figure.1.

4.4. Development of CU-GdNP and FA-CU-GdNP formulations

CU-GdNP were prepared by desolvation method as reported previously with slight modifications 36. Briefly plain Gd and CU were dissolved in a 20 mL mixture of an ethanol: water (7:3 v/v), this solution was added drop wise into a stirred saline phase (0.9% NaCl) containing 0.5% Pluronic F-68 as stabilizer, after addition, ethanol was removed by evaporation under reduced pressure, centrifuged at 40,000g for 30 min, the supernatant was removed and the pellets were re-suspended in water, centrifuged again and finally, the precipitated CU-GdNP was freeze-dried to obtain purified CU-GdNP. CU-GdNP batches were hardened by the addition of 2 mg gluteraldehyde per mg CU-GdNP by stirring for 2 h at room temperature. The same method was followed for the preparation of FA-CU-GdNP in which FA conjugated Gd have been used instead of plain Gd. The blank NP (FA-GdNP and GdNP) have also been prepared by the same method described above by offing the addition of CU in the procedure.

4.5. ES coating on CU-GdNP and FA-CU-GdNP formulations

The above prepared CU-GdNP was further coated with ES using by oil-in-oil solvent evaporation method using coat: core ratio (2:1) [43]. CU-GdNP was dispersed in 10 mL of coating solution prepared by dissolution of ES in ethanol: acetone (2:1). This above dispersion was then poured in 50 ml of light liquid paraffin containing 1% w/v Span 85. This dispersion was maintained under agitation speed of 600 rpm at room temperature for 3 hours, after which the organic phase was removed under vaccum. The resultant solution was washed with 3×50 ml of n-hexane to remove liquid paraffin and dried to obtain ES-CU-GdNP. ES-FA-CU-GdNP have also been prepared by the same method; mentioned above.

Radiolabeled ES-FA-GdNP bearing technetium 99m–labeled diethylene triamine pentacetate (99mTc-DTPA) were prepared similar to the method as discussed above, and all the components were used in the same quantity, except that the CU was replaced with sodium chloride having radioactive (99mTc-DTPA) tracer adsorbed on its surface.

5. Characterization

5.1 Fourier transforms infrared spectroscopy (FTIR)

The conjugation of FA with Gd was confirmed by FTIR spectrum which has been recorded on FTIR multiscope spectrophotometer (Perkin-Elmer, Seer Green, Beaconsfield, and Buckinghamshire, United Kingdom) equipped with spectrum v3.02 software.

5.2 NMR Spectroscopy

The FA conjugation with Gd was further confirmed by NMR spectra by 1H NMR Spectroscopy (Bruker 400 ultrasheild, Switzerland) using the software Topspin.

5.3 Differential Scanning Calorimetry (DSC)

The compatibility of CU with Gd has been established by performing DSC with a Perkin–Elmer DSC apparatus (Perkin–Elmer, Wellesley, MA). Samples were weighed and placed in a 30 µL hermetic aluminum pan and sealed. The sample was scanned at a temperature range of 10°C to 200°C using a heating rate of 5°C/min in a nitrogen atmosphere (flow rate, 10 ml/min).

5.4 Particle size, zeta potential and poly dispersity index

The mean particle size, size distribution and zeta potential of ES-GdNP, ES-FA-GdNP, ES-CU-GdNP and ES-FA-CU-GdNP were determined by a Malvern Zetasizer NanoZS (Malvern 3000HS, France). Each sample was measured in triplicate.

5.5 Entrapment efficiency (% EE)

The amount of the CU entrapped within ES-CU-GdNP and ES-FA-CU-GdNP were determined by ultracentrifugation method. 10 mg of lyophilized ES-CU-GdNP or ES-FA-CU-GdNP were suspended separately in 10 ml of PBS and centrifuged at 60,000 rpm for 3 hours at 4oC. ES-CU-GdNP and ES-FA-CU-GdNP were settled as a pellet and supernatant was analyzed for free CU using RP-HPLC at 425 nm [44]. %EE was calculated from the amount of CU in supernatant and total amount of CU taken for loading. The %EE was determined as follows:

$$\% \text{ E.E} = [(Wi-Wf)/Wi] \times 100$$

Where, Wi, weight of initial drug and Wf is weight of free (un-entrapped) drug.

5.6 Transmission Electron Microscope (TEM)

The characterization of ES-FA-CU-GdNP was carried out by TEM. A drop of the NP suspended in triple distilled water, was placed onto a carbon-coated copper grid, forming a thin liquid film. The films on the grid were negatively stained with a drop of 1% (w/v) phosphotungstic acid. The excess staining solution was removed by filter paper and the sample was then air-dried. These samples were viewed under TEM and photographed.

5.7 HPLC Analysis

A validated RP-HPLC method was developed for estimating CU content in ES-CU-GdNP and ES-FA-CU-GdNP. The HPLC system was equipped with two 10 ATVP binary gradient pumps (Shimadzu), Rheodyne (Cotati, CA, USA) model 7125 injector fitted with a 20 µl loop and SPD-M10 AVP UV detector (Shimadzu). HPLC separation was achieved on a RP-C18 column (250mm, 4.6mm, 5 µm, Merck). Column effluents were monitored at 425 nm. Data was acquired and processed using Shimadzu class VP software. The mobile phase was a mixture of acetonitrile: water: glacial acetic acid (650:340:10) v/v. The solution was filtered and degassed before use. Chromatography was performed at 25°C with a flow rate of 1.0 ml/min. Calibration curve of CU was in the range of 1-10 µg/mL. Under these conditions the drug shows retention time of about 4 min.

5.8 *In vitro* release study

In order to evaluate the difference in the release pattern of the prepared NP, the in vitro release study of CU, ES-CU-GdNP and ES-FA-CU-GdNP was performed in simulated gastric fluid (SGF) at pH 1.2 (2 h), in simulated intestinal fluid (SIF) at pH 7.4 (6 h) and simulated colonic fluids (SCF) of pH 6.8 (24 h) at 37°C [39]. The SGF (pH 1.2) contained sodium chloride (1.0 g), pepsin (1.6 g) and hydrochloric acid (3.5 ml) volume made up to 500 ml with triple distilled water. The SIF (pH 7.4) consisted of monobasic potassium phosphate (3.4 g), 0.2N sodium hydroxide (90 ml) and pancreatin (5 g) and volume made up to 500 ml with triple distilled water. SCF was prepared by a method reported earlier [45, 46].

The release studies were carried out in a USP dissolution test apparatus (Apparatus II, 100 rpm, 37±0.5°C). Briefly, 500 ml of dissolution medium was taken in the container, immersed in the water bath of the apparatus. The activated dialysis bag containing CU, ES-CU-GdNP and ES-FA-CU-GdNP were first immersed in the dissolution medium separately; containing SGF, then into SIF and finally in to SCF. For the release study, Tween 80 (1%, v/v) was added to the dissolution medium to facilitate the CU released from ES-CU-GdNP and ES-FA-CU-GdNP. Samples (2 ml) were withdrawn from each dissolution medium at different time intervals (1, 2, 3, 4, 5, 6, 8, 12, 24 h). The perfect sink condition was maintained by replacing with same volume of respective dissolution medium after each sampling. The sample was centrifuged at 10,000 rpm for 15 min, supernatant was filtered through 0.4 µm membrane filter and the filtrate was subjected to HPLC analysis after appropriate dilution by the method reported above.

5.9 *In vitro* uptake study

The Caco-2 cell line was used for uptake studies of ES-FA-CU-GdNP and ES-CU-GdNP and was evaluated using fluorescence activated cell sorter (FACS) instrument (BD Biosciences, FACS Aria, and Germany). Aliquots (100µL) containing Caco-2 (1 × 105) cells suspended in 0.9ml of fresh RPMI-1640 medium supplemented with penicillin 10 U/ml, 10% FBS, 100µg/ml streptomycin, 1mM sodium pyruvate, and 10 mM HEPES medium. These were transferred into 24-well plates containing fresh medium and suspended in a 37°C humidified incubator with 5% CO2 atmosphere. After 24 h the culture medium was replaced with fresh culture medium. Fluorescein isothiocynate (FITC) loaded ES-CU-GdNP (ES-FITC-GdNP) and FITC loaded ES-FA-CU-GdNP (ES-FA-FITC-GdNP), which was prepared by the same method used for the preparation of ES-CU-GdNP and ES-FA-CU-GdNP as described above, FITC was taken instead of CU. All the protocol was performed in dark conditions. ES-FITC-GdNP and ES-FA-FITC-GdNP containing equivalent amount of CU were added to it in triplicate and incubated for 4 h at room temperature in dark. The cells were scraped and the extent of ES-FITC-GdNP and ES-FA-FITC-GdNP uptake was examined by flow cytometry. The cell-associated fluorescence was measured by FACS at an excitation wavelength of 480 nm and an emission wavelength of 550 nm [47].

5.10 Annexin V/Propidium Iodide staining for apoptotic cells

Quantitation of apoptotic cells by Annexin V staining was performed by according to the manufacturer's instructions (Calbiochem). Briefly, caco-2 cells (5×105cells/well) were seeded in 6 well plates and treated with 5mM of formulations i.e. control, plain drug, ES-CU-GdNP and ES-FA-CU-GdNP for 24 h. After the incubations, cells arranged as a suspension in 500mL of cold PBS, centrifuged for 5 min at 1000 ×g then resuspended in 500 mL cold × binding buffer and added 1.25mL of Annexin V-FITC and incubated for 15 min at RT in dark, centrifuge at 1000 × g for 5 min at RT, discard supernatant, gently resuspend in 500 mL cold × binding buffer and added 10mL PI. Flow cytometry was performed using a FACScan (Becton Dickinson, Mountain View, CA) flow cytometer, equipped with a single 488 nm argon laser. Annexin V-FITC was analyzed using excitation and emission settings of 488 nm and 535 nm (FL-1 channel); PI, 488 nm and 610 nm (FL-2 channel). Debris and clumps were gated out using forward and orthogonal light scatter. The experiment was repeated three times independently. Values are expressed as mean ± SEM.

5.11 Cytotoxicity study

In vitro cytotoxicity of CU, ES-CU-GdNP and ES-FA-CU-GdNP were analyzed in Caco-2 cell lines by (3-(4,5-dimethylthiazol-2-yl)-2,5-diphenyl tetrazolium bromide) MTT assay. Caco-2 cell line was maintained as described above. The Caco-2 cells were seeded onto 96 well plates at a density of 4×105cells/well for 24 h and CU, ES-CU-GdNP and ES-FA-CU-GdNP at a equivalent concentration of CU i.e. 1 µM, 10µM, 25µM and 50µM were incubated for 24 h [48]. Blank formulations ES-Gd-NP and ES-FA-GdNP at all equivalent concentration were also incubated [49]. Cytotoxicity was estimated by staining live cell by 0.5 mg/mL MTT for 3 h (formazan crystal formation), the optical density values were determined at 540 nm using ELISA plate reader. Triplicates of each sample were analyzed.

5.12 In vivo studies

5.13.1 *In vivo* tumor xenograft study

The in-vivo anti-tumor cancer targeting efficacy of the ES-FA-CU-GdNP was assessed in the tumor bearing Male nude mice of 3-4 weeks by assembly these mice were immunodefficient via irradiation. The HCT-116 2 × 106 cancer cells/mice were applied intraperitoneally in 1 mL culture medium by sterile injection. After 2 weeks, all of the animals had developed intra abdominal tumor nodes. They were used as tumor bearing mice for the solid colon cancer model [50, 51]. All procedures were performed in a laminar flow hood using aseptic techniques. The initial tumor size was taken approximately 100 mm3 in size. The tumor bearing mice were randomly divided into four treatment groups (control, free CU, ES-CU-GdNP and ES-FA-CU-GdNP) for treatment with 25 mg/kg body weight dose equivalent to CU. At predetermined time intervals the tumor volume (mm3) was measured by measuring its dimension (major and minor axis) using electronic digital Vernier Caliper and the tumor volume was estimated according to the following formula: tumor volume (mm3) =L×W2 /2, where L is the length and W the width. The study was terminated 35 days post treatment at the end of the experiment and represents the mean ± SD. All animals were accommodated in a pathogen-free laboratory environment during the tenure of the studies.

5.13.2 Plasma and tissue distribution study

The drug distribution profiles of free CU, ES-CU-GdNP. ES-FA-CU-GdNP in various organs/tissues after oral administration were investigated. Healthy Nude tumorigenic mice (male, 30–35 g) were assigned randomly into four groups with 30 mice in each group for this study. The first group served as control. Free CU was given to all mice in the second group, whereas mice of the third and fourth groups received ES-CU-GdNP and ES-FA-CU-GdNP respectively by oral administration. The dose of CU given to animals was equivalent to 25 mg/kg body weight of animals. Three animals from each group were killed at each time point (i.e., 0.5, 1, 2, 3, 4, 6, 8, 10, 12, and 24 hours). The Gastro intestinal tract (GIT) was removed, and the mesenteric and fatty acid tissues were removed. The GIT was fragmented into the stomach, small intestine, and colon. Tumor was also isolated, washed with Ringer's solution to separate any adhered debris and dried using tissue paper and simultaneously the blood was also collected from the heart puncture.

Organs and luminal contents were weighed and homogenized with 2 mL PBS (pH 7.4) using tissue homogenizer (MAC Micro Tissue Homogenizer; New Delhi, India) and vortexed after addition of chloroform (CHCl3) and methanol (CH3OH) mixture and centrifugation for 5 min at 2000 × g on Sigma 3-16K (Frankfurt, Germany). After centrifugation, obtained supernatant was decanted into another eppendrof and evaporated to dryness under vacuum in speed vaccum concentrator (Savant Instrument, Farmingdale, USA). The residue was reconstituted in 50 µL of the mobile phase, vortexed and 20 µL was injected onto analytical column. Concentration of CU in tissues was determined by HPLC, using the method reported previously. Similarly, the blood samples were prepared and analyzed for the drug content using the HPLC method.

5.13.4 γ-Scintigraphic study

The present study was performed to investigate the behavior of drug dosage form and to estimate the release pattern of the NP qualitatively within the GIT of mice. Mice weighing between 30-35 g were selected and fasted overnight before administration of the enteric-coated radiolabeled NP. Now, to evaluate the presence of the radiolabeled NP in different parts of GIT, a high dose (1 mCi) of 99m Tc-DTPA was encapsulated in NP and radioactivity was measured using radioisotope dose calibrator (CRC-127R; Capintech Inc., Pittsburgh, Pennsylvania). These enteric-coated radiolabeled NP were orally administered to the mice with 2 mL of water. The dosed mice were kept in a restraining cage that was located under the scintillation camera. Transit of the radiolabeled NP through the GIT was supervised at different time intervals using a gamma camera (E. Cam Siemens, Germany) fitted with low energy all-purpose collimator for scanning. The camera was connected to a computer system for attainment and storage of data. The useful field of view was 256 × 256 mm, and the mean energy window of 99mTc was 140 ± 14 keV. The camera was set for 100 K counts for each acquisition, and anterior images were recorded with the rodents in supine position. Images were recorded after one hrs administration of the NP and at 10 min intervals for 3 h and then at 20 min intervals up to 6 hrs and later on at 60 min intervals up to the gamma images were recorded for 24 hr study period using an online computer system and analyzed to determine the distribution of activity in the GI tract as demonstrated and archived onto optical disk for subsequent analysis.

6. Statistical analysis

All data are expressed as mean ± standard deviation. Statistical analysis was done with one-way analysis of variance (ANOVA) followed by the Turkey-Kramer multiple comparison test, using Graph Pad Instat software (Graph Pad Software Inc., San Diego, California). A probability $p<0.05$ was considered while significant, $p<0.01$ and $p<0.001$ was considered as extremely significant.

7. Conclusions

It is observed that there is a regression in tumor size after the administration of ES-FA-CU-GdNP. Experimental observations also suggest that ES-FA-CU-GdNP are more effective against the HCT-116 tumor bearing nude mice than free CU and ES-CU-GdNP. The plasma and tissue distribution studies results demonstrate that the maximum amount of CU is recovered from colon and tumor indicating the efficacy of colon specific drug delivery. In addition, since the surface of the ES-CU-GdNP could be similarly functionalized with other targeting ligand besides FA, they should serve as an effective carrier for targeted drug delivery to different types of cancer. ES-FA-CU-GdNP might have potential in cancer diagnosis and therapy which is more affected in FRs expressed on the tumor surface offers the dual advantage of localizing tumors by non-invasive imaging and also treating them.

8. Ethical Statement:

Eight-ten weeks old nude mice (male, 30-35 g) were obtained from INMAS New Delhi, India and were acclimatized in a climate- and light cycle-controlled environment for 2 days before investigation. he animals were maintained at the controlled temperature of 23 ± 1ºC, humidity of 55 ± 5%, in a 14 h light/10 h dark cycle. Throughout the study, the animals were provided with soy-free and filtered drinking water. The animal experiments have been carried out by following experimental protocol guidelines of Council for the Purpose of Control and Supervision of Experiments on Animals (CPCSEA), Ministry of Social Justice and Empowerment, Government of India. Experiments were conducted after ethical clearance by the Institutional Animal Ethics Committee of the institute (INM/DASQA/IAEC/09/015).

9. Acknowledgments

The authors are particularly grateful to SAIF, CDRI, Lucknow, India, for spectral analysis, AIIMS, New Delhi, India for TEM analysis. The author is thankful to ICMR, New Delhi India for providing SRF. This work was supported by a grant from the Indian Council of Medical Research, New Delhi, India. .

10. Conflict of Interest statement

The authors declare they have no competing financial interest.

Notes

[1]*Pharmaceutics Division, Central Drug Research Institute, Lucknow 226031, India.*
[2] *Division of Cyclotron & Radiopharmaceutical Sciences, Institute of Nuclear Medicine and Allied Sciences (INMAS), DRDO, Delhi-110054, India.*

Corresponding author:
Dr. A K Dwivedi, Scientist, Pharmaceutics Division,
CSIR-Central Drug Research Institute, Sector 10, Janki Puram Extention, Sitapur Road, Lucknow, 226031, India
Phone: 9415910144
Email: anilcdri@gmail.com, renukadops@gmail.com

References

1. L. Brannon-Peppas and J. O. Blanchette, *Adv Drug Deliv Rev*, 2004, **56**, 1649-1659.
2. S. S. Feng, *Expert Rev Med Devices*, 2004, **1**, 115-125.
3. M. Das, C. Mohanty and S. K. Sahoo, *Expert Opin Drug Deliv*, 2009, **6**, 285-304.
4. S. K. Sahoo and V. Labhasetwar, *Drug Discov Today*, 2003, **8**, 1112-1120.
5. P. Anand, C. Sundaram, S. Jhurani, A. B. Kunnumakkara and B. B. Aggarwal, *Cancer Lett*, 2008, **267**, 133-164.
6. B. B. Aggarwal, A. Kumar and A. C. Bharti, *Anticancer Res*, 2003, **23**, 363-398.
7. E. Balogun, M. Hoque, P. Gong, E. Killeen, C. J. Green, R. Foresti, J. Alam and R. Motterlini, *Biochem J*, 2003, **371**, 887-895.
8. A. Mazumder, K. Raghavan, J. Weinstein, K. W. Kohn and Y. Pommier, *Biochem Pharmacol*, 1995, **49**, 1165-1170.
9. A. Duvoix, R. Blasius, S. Delhalle, M. Schnekenburger, F. Morceau, E. Henry, M. Dicato and M. Diederich, *Cancer Lett*, 2005, **223**, 181-190.
10. W. M. Abuzeid, S. Davis, A. L. Tang, L. Saunders, J. C. Brenner, J. Lin, J. R. Fuchs, E. Light, C. R. Bradford, M. E. Prince and T. E. Carey, *Arch Otolaryngol Head Neck Surg*, 2011, **137**, 499-507.
11. S. V. Bava, V. T. Puliappadamba, A. Deepti, A. Nair, D. Karunagaran and R. J. Anto, *J Biol Chem*, 2005, **280**, 6301-6308.
12. L. Li, B. Ahmed, K. Mehta and R. Kurzrock, *Mol Cancer Ther*, 2007, **6**, 1276-1282.
13. N. K. Narayanan, D. Nargi, C. Randolph and B. A. Narayanan, *Int J Cancer*, 2009, **125**, 1-8.
14. K. Maiti, K. Mukherjee, A. Gantait, B. P. Saha and P. K. Mukherjee, *Int J Pharm*, 2007, **330**, 155-163.
15. M. M. Yallapu, M. Jaggi and S. C. Chauhan, *Macromol Biosci*, 2010, **10**, 1141-1151.
16. S. Bisht, G. Feldmann, S. Soni, R. Ravi, C. Karikar and A. Maitra, *J Nanobiotechnology*, 2007, **5**, 3.
17. A. O. Elzoghby, W. S. El-Fotoh and N. A. Elgindy, *J Control Release*, 2011, **153**, 206-216.
18. Y. Lu and S. C. Chen, *Adv Drug Deliv Rev*, 2004, **56**, 1621-1633.
19. C. Coester, P. Nayyar and J. Samuel, *Eur J Pharm Biopharm*, 2006, **62**, 306-314.
20. I. Ezpeleta, M. A. Arangoa, J. M. Irache, S. Stainmesse, C. Chabenat, Y. Popineau and A. M. Orecchioni, *Int J Pharm*, 1999, **191**, 25-32.
21. C. Duclairoir, A. M. Orecchioni, P. Depraetere, F. Osterstock and E. Nakache, *Int J Pharm*, 2003, **253**, 133-144.
22. R. B. Umamaheshwari, S. Ramteke and N. K. Jain, *AAPS PharmSciTech*, 2004, **5**, e32.
23. Y. Zhang, N. Kohler and M. Zhang, *Biomaterials*, 2002, **23**, 1553-1561.
24. E. K. Park, S. B. Lee and Y. M. Lee, *Biomaterials*, 2005, **26**, 1053-1061.
25. M. O. Oyewumi, R. A. Yokel, M. Jay, T. Coakley and R. J. Mumper, *J Control Release*, 2004, **95**, 613-626.
26. S. Mansouri, Y. Cuie, F. Winnik, Q. Shi, P. Lavigne, M. Benderdour, E. Beaumont and J. C. Fernandes, *Biomaterials*, 2006, **27**, 2060-2065.
27. P. Chan, M. Kurisawa, J. E. Chung and Y. Y. Yang, *Biomaterials*, 2007, **28**, 540-549.
28. Y. Lu and P. S. Low, *Adv Drug Deliv Rev*, 2002, **54**, 675-693.
29. J. Sudimack and R. J. Lee, *Adv Drug Deliv Rev*, 2000, **41**, 147-162.
30. S. Wang and P. S. Low, *J Control Release*, 1998, **53**, 39-48.
31. J. F. Kukowska-Latallo, K. A. Candido, Z. Cao, S. S. Nigavekar, I. J. Majoros, T. P. Thomas, L. P. Balogh, M. K. Khan and J. R. Baker, Jr., *Cancer Res*, 2005, **65**, 5317-5324.
32. Y. Liu, K. Li, J. Pan, B. Liu and S. S. Feng, *Biomaterials*, 2010, **31**, 330-338.
33. M. He, Z. Zhao, L. Yin, C. Tang and C. Yin, *Int J Pharm*, 2009, **373**, 165-173.
34. M. Gulfam, J.-e. Kim, J. M. Lee, B. Ku, B. H. Chung and B. G. Chung, *Langmuir*, 2012, **28**, 8216-8223.
35. C. V. Rao and B. S. Reddy, *Curr Cancer Drug Targets*, 2004, **4**, 29-42.
36. M. A. Arangoa, G. Ponchel, A. M. Orecchioni, M. J. Renedo, D. Duchene and J. M. Irache, *Eur J Pharm Sci*, 2000, **11**, 333-341.
37. C. M. Paulos, J. A. Reddy, C. P. Leamon, M. J. Turk and P. S. Low, *Mol Pharmacol*, 2004, **66**, 1406-1414.
38. Y. Liu, K. Li, J. Pan, B. Liu and S.-S. Feng, *Biomaterials*, 2010, **31**, 330-338.
39. M. Sharma, R. L. Salisbury, E. I. Maurer, S. M. Hussain and C. E. Sulentic, *Nanoscale*, 2013.
40. J. Pan and S.-S. Feng, *Biomaterials*, 2008, **29**, 2663-2672.
41. J. G. Hardy, S. S. Davis, R. Khosla and C. S. Robertson, *International journal of pharmaceutics*, 1988, **48**, 79-82.
42. V. P. Fitzjarrald and R. Pongdee, *Tetrahedron Letters*, 2007, **48**, 3553-3557.
43. T. Oosegi, H. Onishi and Y. Machida, *European Journal of Pharmaceutics and Biopharmaceutics*, 2008, **68**, 260-266.
44. T. Sartori, F. Seigi Murakami, A. Pinheiro Cruz and A. Machado de Campos, *J Chromatogr Sci*, 2008, **46**, 505-509.
45. Y. S. Krishnaiah, V. Satyanarayana, B. Dinesh Kumar and R. S. Karthikeyan, *Eur J Pharm Sci*, 2002, **16**, 185-192.
46. V. R. Sinha, B. R. Mittal, K. K. Bhutani and R. Kumria, *Int J Pharm*, 2004, **269**, 101-108.

47. R. Khatik, R. Mishra, A. Verma, P. Dwivedi, V. Kumar, V. Gupta, S. Paliwal, P. Mishra and A. Dwivedi, *J Nanopart Res*, 2013, **15**, 1-15.
48. P. Dwivedi, S. Kansal, M. Sharma, R. Shukla, A. Verma, P. Shukla, P. Tripathi, P. Gupta, D. Saini, K. Khandelwal, R. Verma, A. K. Dwivedi and P. R. Mishra, *J Drug Target*, 2012, **20**, 883-896.
49. S. K. Sahoo, W. Ma and V. Labhasetwar, *Int J Cancer*, 2004, **112**, 335-340.
50. K. Flatmark, G. M. Mælandsmo, M. Martinsen, H. Rasmussen and Ø. Fodstad, *European Journal of Cancer*, 2004, **40**, 1593-1598.
51. E. E. Ibrahim, R. Babaei-Jadidi, A. Saadeddin, B. Spencer-Dene, S. Hossaini, M. Abuzinadah, N. Li, W. Fadhil, M. Ilyas, D. Bonnet and A. S. Nateri, *STEM CELLS*, 2012, **30**, 2076-2087.

Figure 1. Schematic diagram showing conjugation of FA with Gd.

Figure 2. FT-IR spectra of FA conjugated Gd.

Figure 3: NMR Spectra of FA conjugated Gd.

Figure 4: Compatibility of Gd and CU by DSC.

Figure 5: TEM images of ES-FA-CU-GdNP

Figure 6: *In vitro* drug release profile of CU, ES-CU-GdNP and ES-FA-CU-GdNP in different gastro intestinal simulated fluids (SGF, SIF, and SCF).

Figure 7: Flow cytometric uptake studies in caco-2 cells. X-axis represents florescence inside the cells. Figure shows florescence in (i) control cells (ii) ES-FITC-GdNP, (iii) ES-FA-FITC-GdNP. **$p<0.001$.

Figure 8: Apoptotic cells detected by flow cytometry with Annexin V conjugated with PI staining on caco-2 cells were treated with different formulation (A) control (B) Plain CU (C) ES-CU-GdNP and (D) ES-FA-CU-GdNP.

Figure 9: % Cell cytoxicity of Caco-2 cells exposed to 5 µM, 10 µM, 20 µM and 40 µM equivalent concentration of CU in the plain CU, ES-CU-GdNP and ES-FA-CU-GdNP.

Figure 10: *In-vivo* bioavailability of CU, ES-CU-GdNP and ES-FA-CU-GdNP. Values are mean ± SD (n = 3)

Figure 11: Distribution profiles of CU, ES-CU-GdNP and ES-FA-CU-GdNP in various tissues as a function of time after oral dose (25mg/kg) to mice represent mean ± SD obtained from three animals per time point. Colon (+C)*, includes colon contents and tissue, cecal contents, and tissue; CU; curcumin, SI; small intestine.

Figure 12: Gamma scintigraphy captured at different time intervals following oral administration of NP (a) Gamma scintigraph at 1 hr showing the release of negligible amount of

tracer in stomach from enteric coated NP. (b) Gamma scintigraph at 3 hr showing the release of tracer in ascending colon form enteric coated NP. (c) Gamma scintigraph at 6 hr showing the release of tracer in ascending colon and entry of NP mass into transverse colon. (d) Gamma scintigraph at 12 hr showing the distribution of liberated radioactivity in whole colon from enteric coated NP. (e) Gamma scintigraph at 24 hr showing the radioactivity in distal part of colon from enteric coated NP.

Figure 13: (A) Body weight changes in tumor bearing nude mice after administration of CU solution and CU loaded NP formulations, (B) Tumor regression analysis after oral administration of control, CU, ES-CU-GdNP and ES-FA-CU-GdNP (25 mg/kg body weight dose). The ES-FA-CU-GdNP treated group showed suppression of tumor growth compared with the other groups (lower) (n=3).

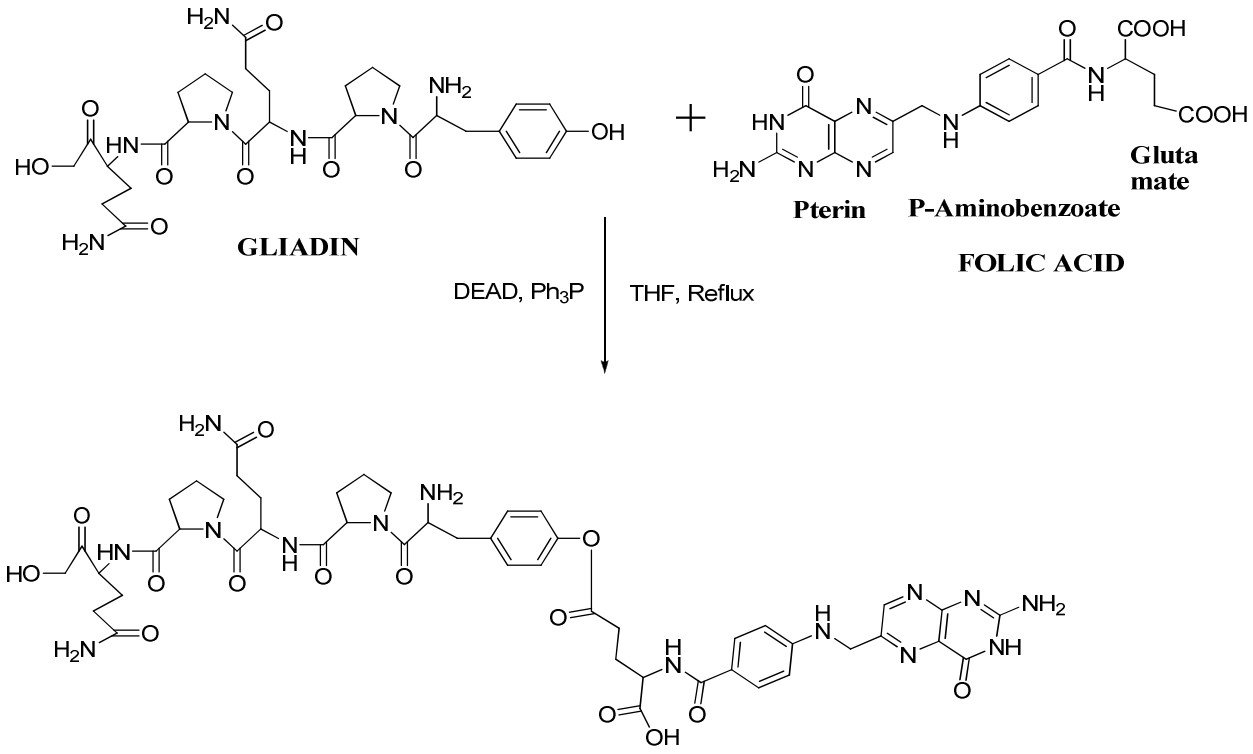

Figure 1. Schematic diagram showing conjugation of FA with Gd.

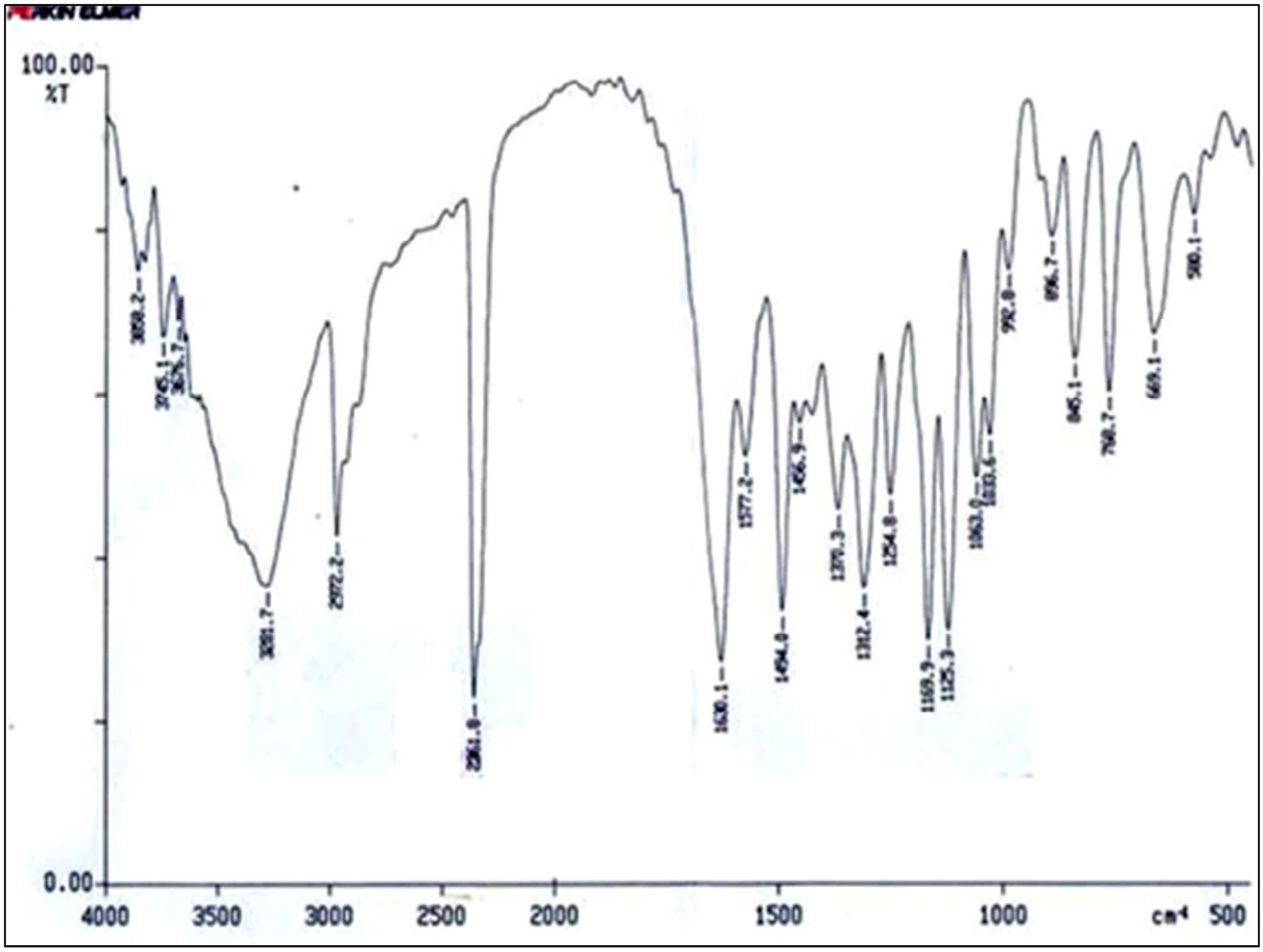

Figure 2. FT-IR spectra of FA conjugated Gd.

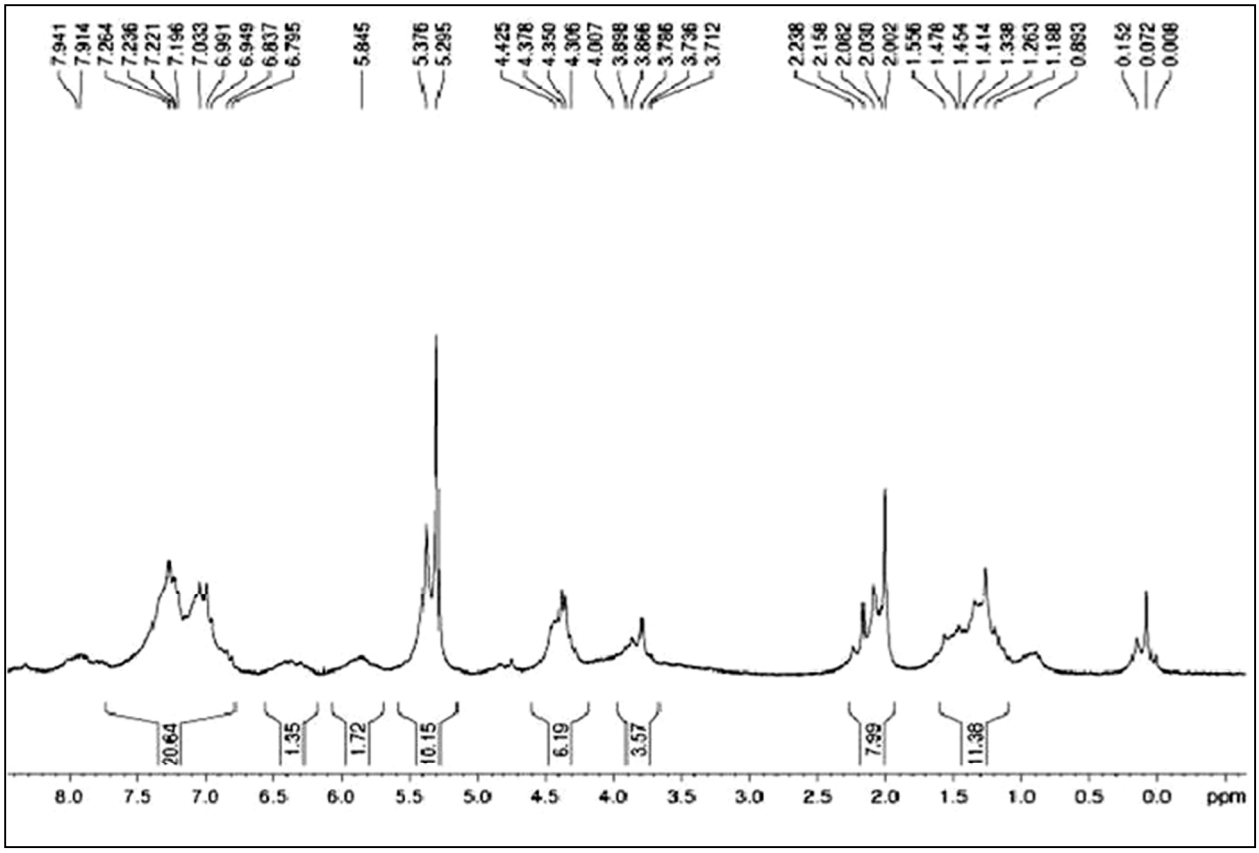

Figure 3: NMR Spectra of FA conjugated Gd.

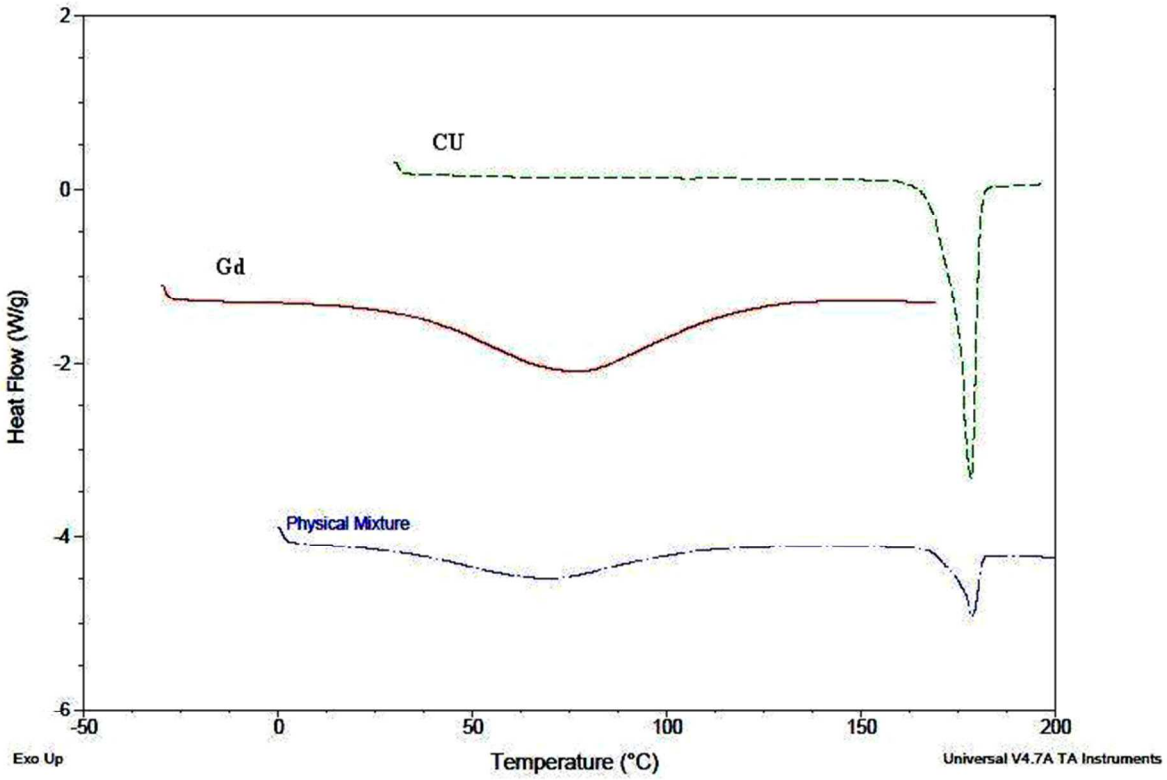

Figure 4: Compatibility of Gd and CU by DSC.

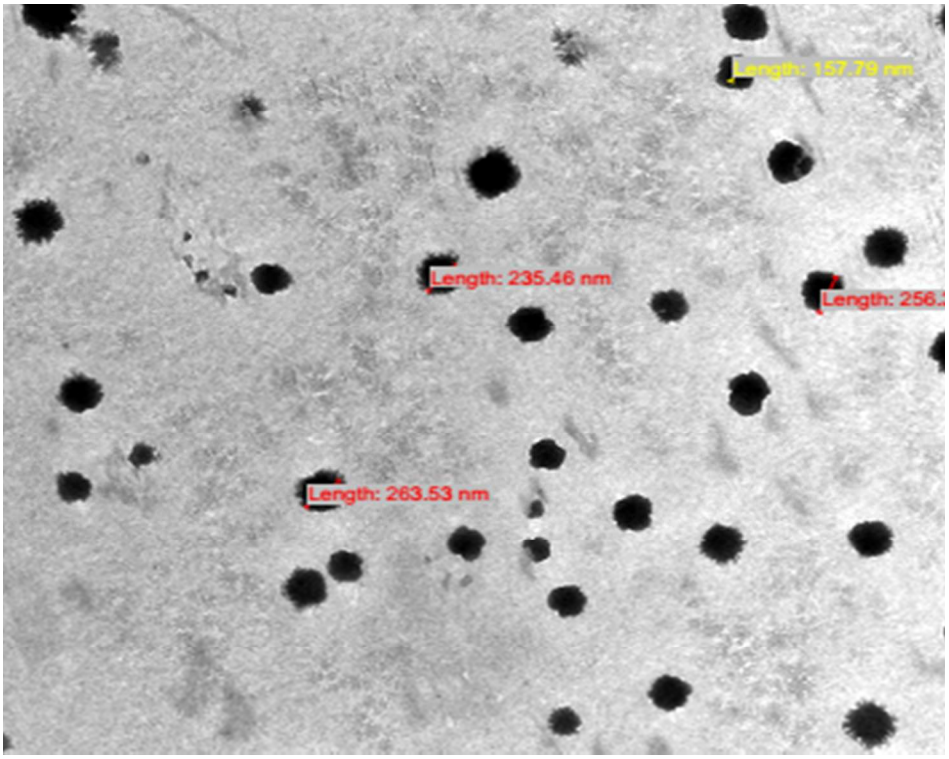

Figure 5: TEM images of ES-FA-CU-GdNP

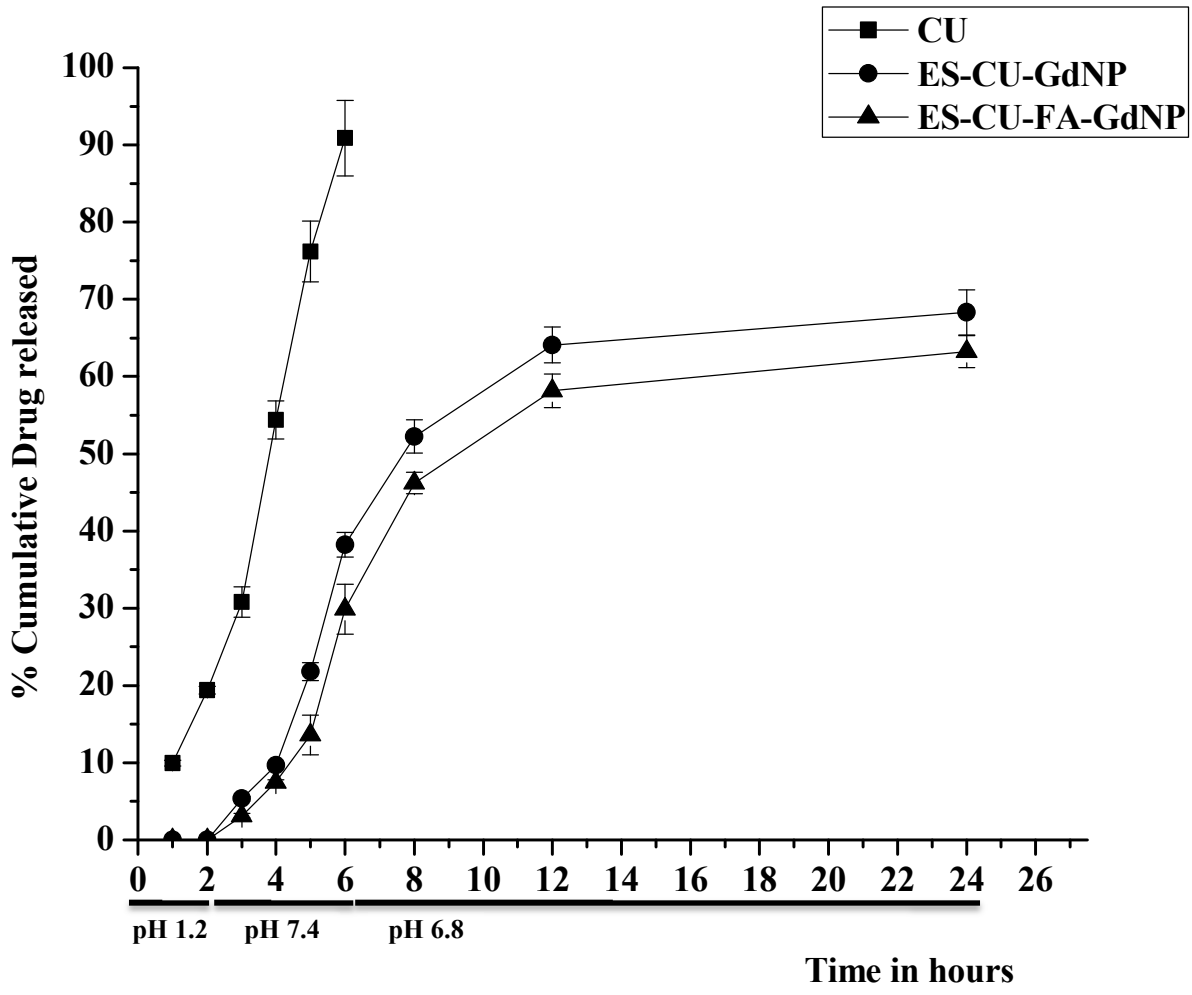

Figure 6: *In vitro* drug release profile of CU, ES-CU-GdNP and ES-FA-CU-GdNP in different gastro intestinal simulated fluids (SGF, SIF, and SCF).

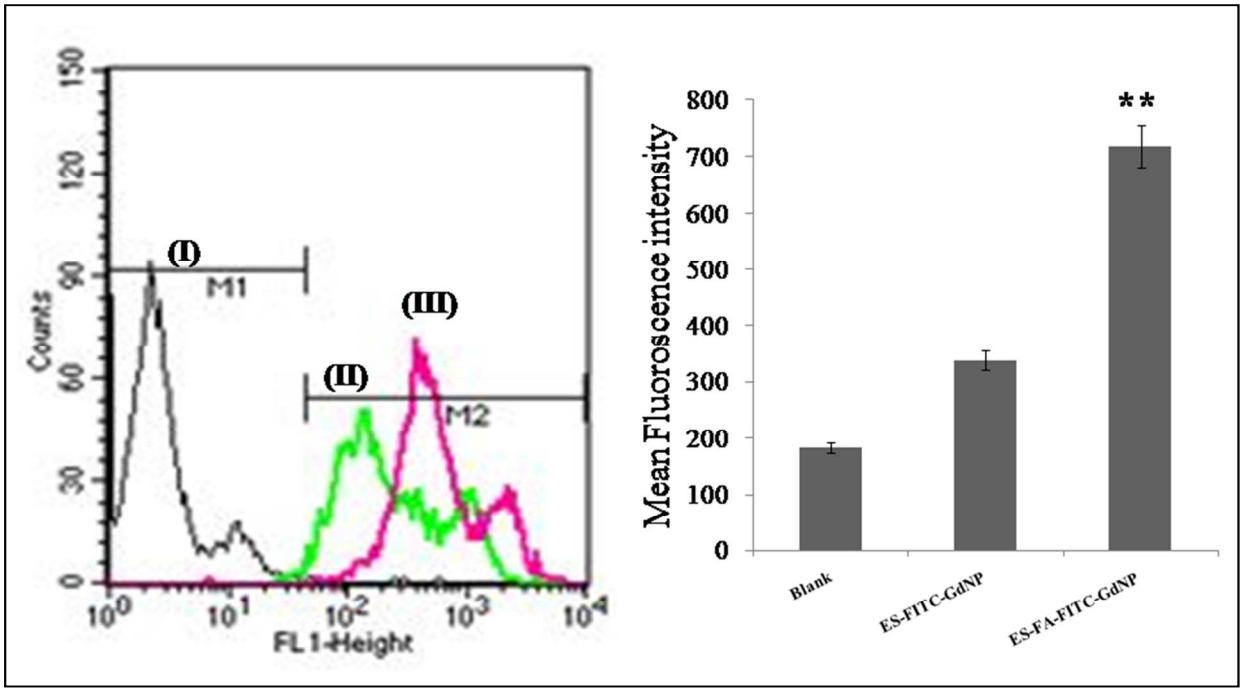

Figure 7: Flow cytometric uptake studies in caco-2 cells. X-axis represents florescence inside the cells. Figure shows florescence in (i) control cells (ii) ES-FITC-GdNP, (iii) ES-FA-FITC-GdNP. **p<0.001.

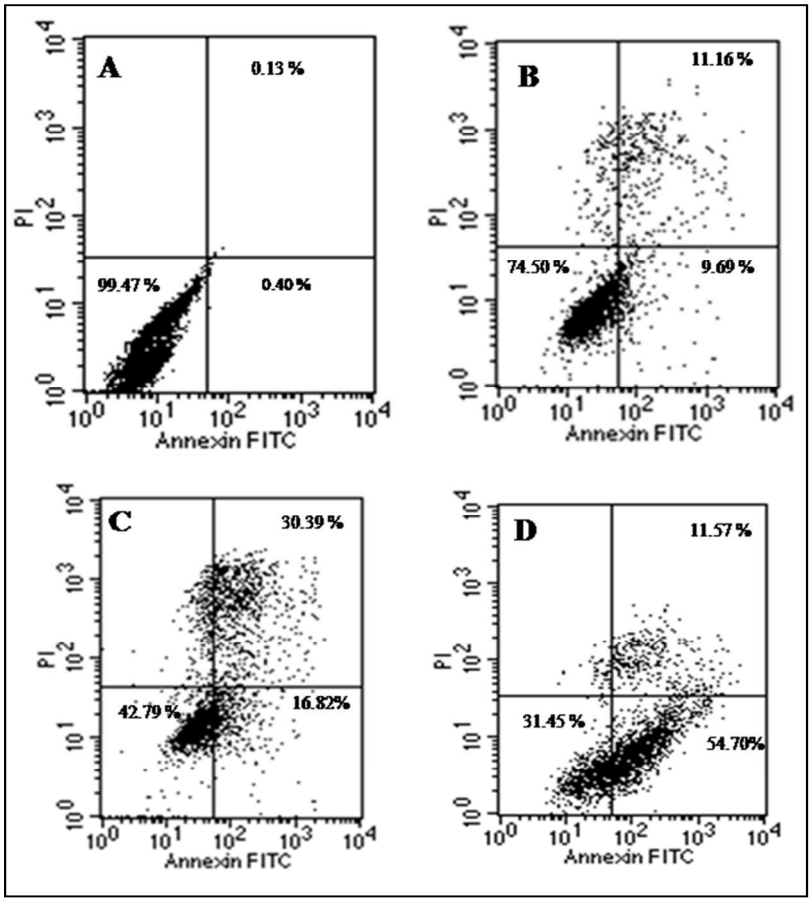

Figure 8: Apoptotic cells detected by flow cytometry with Annexin V conjugated with PI staining on caco-2 cells were treated with different formulation (A) control (B) Plain CU (C) ES-CU-GdNP and (D) ES-FA-CU-GdNP.

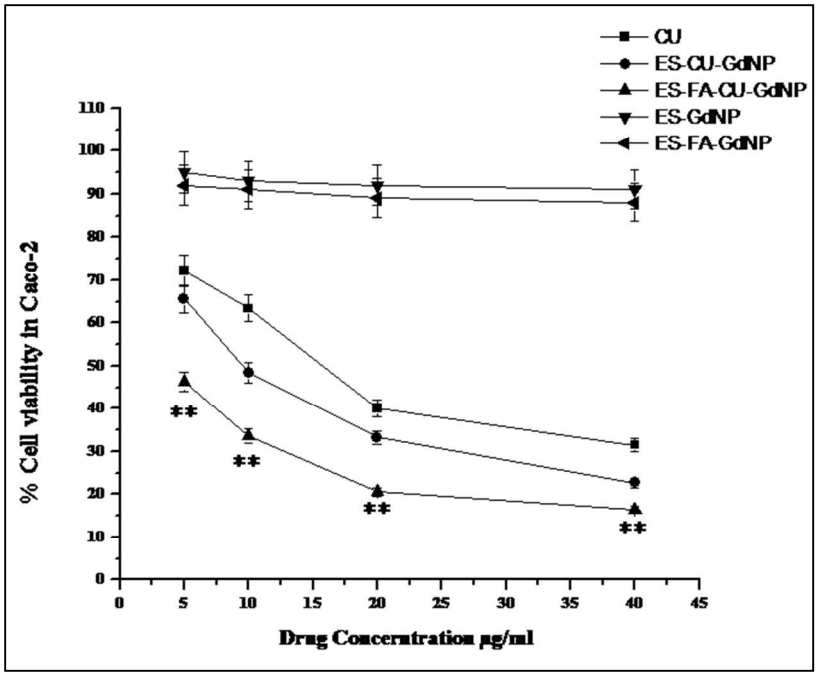

Figure 9: % Cell cytoxicity of Caco-2 cells exposed to 5 µM, 10 µM, 20 µM and 40 µM equivalent concentration of CU in the plain CU, ES-CU-GdNP and ES-FA-CU-GdNP.

Values shown are means and standard deviations (n=3), **p<0.001.

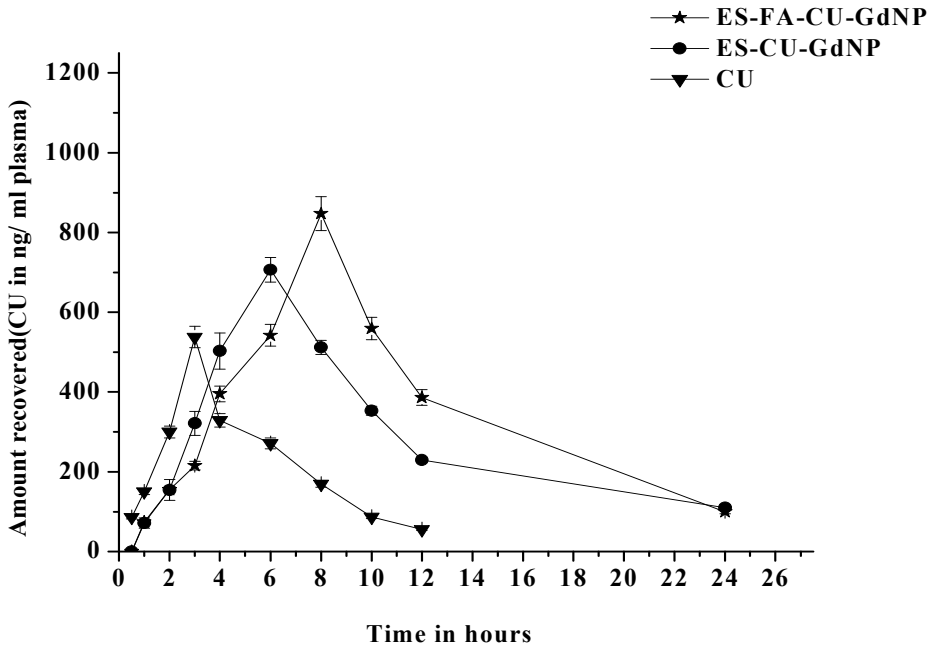

Figure 10: *In-vivo* bioavailability of CU, ES-CU-GdNP and ES-FA-CU-GdNP. Values are mean ± SD (n = 3)

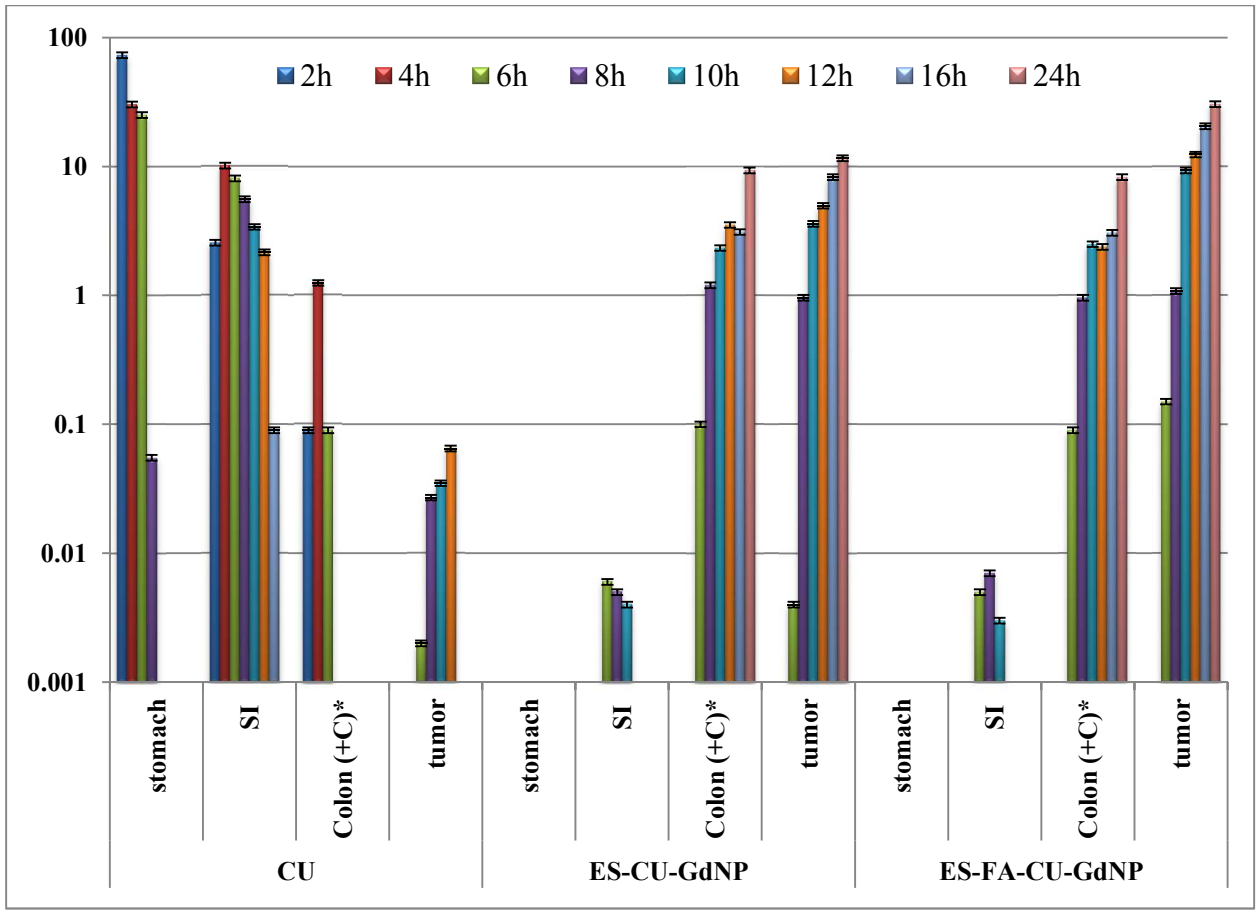

Figure 11: Distribution profiles of CU, ES-CU-GdNP and ES-FA-CU-GdNP in various tissues as a function of time after oral dose (25mg/kg) to mice represent mean ± SD obtained from three animals per time point. Colon (+C)*, includes colon contents and tissue, cecal contents, and tissue; CU; curcumin, SI; small intestine.

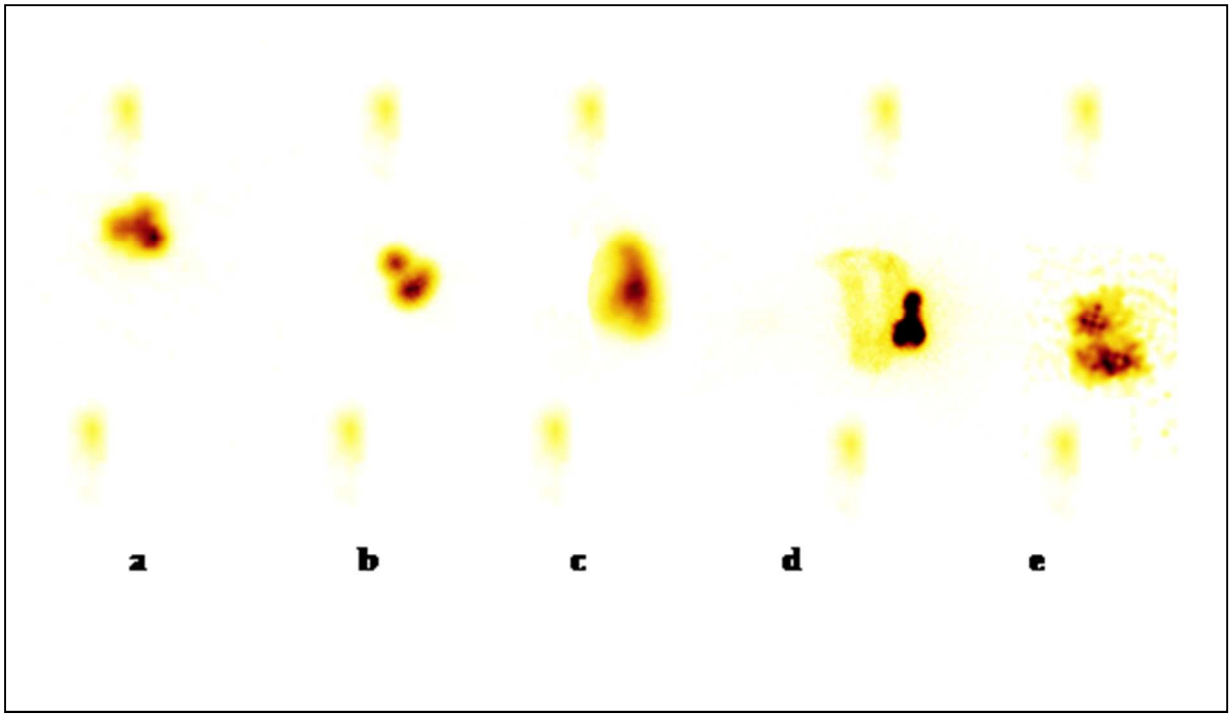

Figure 12: Gamma scintigraphy captured at different time intervals following oral administration of NP (a) Gamma scintigraph at 1 hr showing the release of negligible amount of tracer in stomach from enteric coated NP. (b) Gamma scintigraph at 3 hr showing the release of tracer in ascending colon form enteric coated NP. (c) Gamma scintigraph at 6 hr showing the release of tracer in ascending colon and entry of NP mass into transverse colon. (d) Gamma scintigraph at 12 hr showing the distribution of liberated radioactivity in whole colon from enteric coated NP. (e) Gamma scintigraph at 24 hr showing the radioactivity in distal part of colon from enteric coated NP.

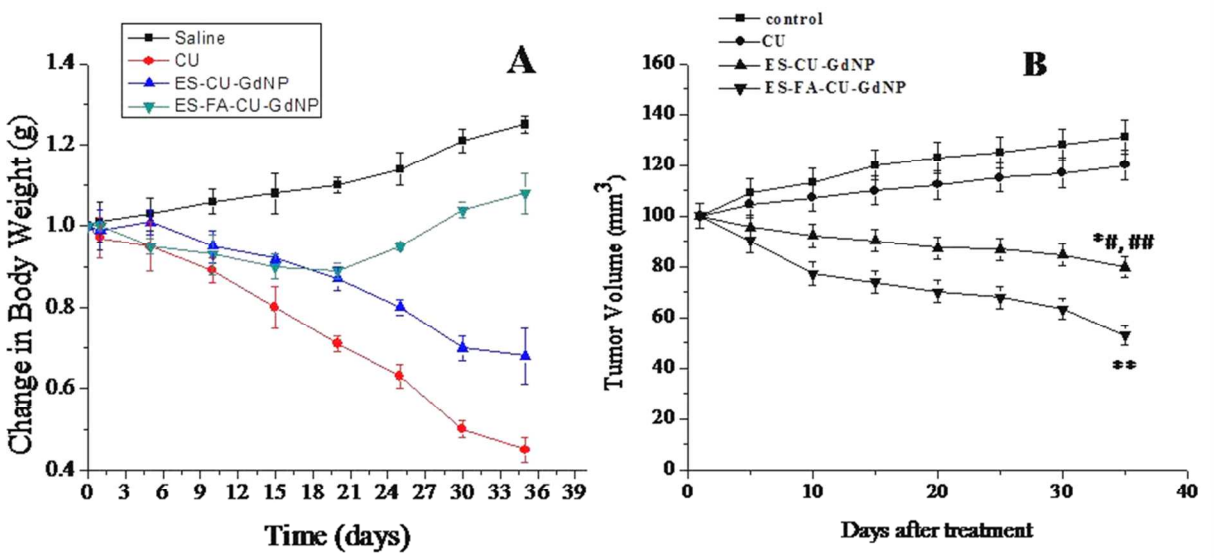

Figure 13: (A) Body weight changes in tumor bearing nude mice after administration of CU solution and CU loaded NP formulations, (B) Tumor regression analysis after oral administration of control, CU, ES-CU-GdNP and ES-FA-CU-GdNP (25 mg/kg body weight dose). The ES-FA-CU-GdNP treated group showed suppression of tumor growth compared with the other groups (lower) (n=3). (**P < 0.001 for ES-FA-CU-GdNP versus control and CU). (* # P<0.01 for ES-CU-GdNP versus control and ## P<0.05 Depicts comparison of ES-CU-GdNP versus CU.

Table 1 : Physicochemical characterization of different GdNP (Values represented as mean ± SD; n=3).

Formulation	Particle Size (nm)± SD	PDI	Zeta potential (mV) ± ZD	%Entrapment efficacy
ES-FA-CU- GdNP	249.3(7.2)	0.175	-27.1(1.8)	53.2 (4.1)
ES-CU-GdNP	137.2(4.1)	0.191	-10.7(2.0)	49.4 (3.8)
ES-GdNP	98.3 (3.5)	0.131	- 8.3 (1.2)	-
ES-FA-GdNP	112.4 (8.6)	0.127	-21.3 (1.6)	-

Table: 2. Pharmacokinetic parameters of CU upon oral administration of CU, ES-CU-GdNP and ES-FA-CU-GdNP.

Formulation	Cmax (ng/ml)	Tmax (hrs)	$AUC_{0-\infty}$(ng/h/ml)	MRT (hrs)
CU	537.47± 15.05	3±014	2794.44±61.13	5.655±2.57
ES-CU-GdNP	706.7±24.89	6±0.09	8123.57±85.1**	11.4301±2.14
ES-FA-CU-GdNP	847.067±29.67	8±1.28	10837.5±102.34** ##	14.65571±3.52

Cmax: maximal plasma concentration, Tmax: time to reach maximal plasma concentration, AUC: area under plasma concentration versus time curve, MRT: mean residual time.

** $p<0.01$ Significances vs. CU, ## $p<0.01$ denotes ES-FA-CU-GdNP vs. ES-FA-CU-GdNP